

Article

A Jug-Shaped CPW-Fed Ultra-Wideband Printed Monopole Antenna for Wireless Communications Networks

Sarosh Ahmad ^{1,2,*} , Umer Ijaz ² , Salman Naseer ³ , Adnan Ghaffar ⁴ , Muhammad Awais Qasim ²,
Faisal Abrar ² , Naser Ojaroudi Parchin ^{5,*} , Chan Hwang See ⁵  and Raed Abd-Alhameed ⁶ 

¹ Department of Signal Theory and Communications, Universidad Carlos III de Madrid, Leganes, 28911 Madrid, Spain

² Department of Electrical Engineering and Technology, Government College University Faisalabad (GCUF), Faisalabad 38000, Pakistan; umer.ijaz@gcu.edu.pk (U.I.); imawais16@gmail.com (M.A.Q.); imfaisalabrar@gmail.com (F.A.)

³ Department of Information Technology, University of the Punjab Gujranwala Campus, Gujranwala 52250, Pakistan; salman@pugc.edu.pk

⁴ Department of Electrical and Electronic Engineering, Auckland University of Technology, Auckland 1010, New Zealand; aghaffar@aut.ac.nz

⁵ School of Engineering and the Built Environment, Edinburgh Napier University, Edinburgh EH14 1DJ, UK; C.See@napier.ac.uk

⁶ Faculty of Engineering and Informatics, University of Bradford, Bradford BD7 1DP, UK; r.a.a.abd@bradford.ac.uk

* Correspondence: saroshahmad@ieee.org (S.A.); N.OjaroudiParchin@napier.ac.uk (N.O.P.)

Abstract: A type of telecommunication technology called an ultra-wideband (UWB) is used to provide a typical solution for short-range wireless communication due to large bandwidth and low power consumption in transmission and reception. Printed monopole antennas are considered as a preferred platform for implementing this technology because of its alluring characteristics such as light weight, low cost, ease of fabrication, integration capability with other systems, etc. Therefore, a compact-sized ultra-wideband (UWB) printed monopole antenna with improved gain and efficiency is presented in this article. Computer simulation technology microwave studio (CSTMWS) software is used to build and analyze the proposed antenna design technique. This broadband printed monopole antenna contains a jug-shaped radiator fed by a coplanar waveguide (CPW) technique. The designed UWB antenna is fabricated on a low-cost FR-4 substrate with relative permittivity of 4.3, loss tangent of 0.025, and a standard height of 1.6 mm, sized at 25 mm × 22 mm × 1.6 mm, suitable for wireless communication system. The designed UWB antenna works with maximum gain (peak gain of 4.1 dB) across the whole UWB spectrum of 3–11 GHz. The results are simulated, measured, and debated in detail. Different parametric studies based on numerical simulations are involved to arrive at the optimal design through monitoring the effects of adding cuts on the performance of the proposed antennas. Therefore, these parametric studies are optimized to achieve maximum antenna bandwidth with relatively best gain. The proposed patch antenna shape is like a jug with a handle that offers greater bandwidth, good gain, higher efficiency, and compact size.

Keywords: printed monopole; CPW-fed; UWB; wireless communication



Citation: Ahmad, S.; Ijaz, U.; Naseer, S.; Ghaffar, A.; Qasim, M.A.; Abrar, F.; Parchin, N.O.; See, C.H.; Abd-Alhameed, R. A Jug-Shaped CPW-Fed Ultra-Wideband Printed Monopole Antenna for Wireless Communications Networks. *Appl. Sci.* **2022**, *12*, 821. <https://doi.org/10.3390/app12020821>

Academic Editor: Amalia Miliou

Received: 8 December 2021

Accepted: 12 January 2022

Published: 14 January 2022

Publisher's Note: MDPI stays neutral with regard to jurisdictional claims in published maps and institutional affiliations.



Copyright: © 2022 by the authors. Licensee MDPI, Basel, Switzerland. This article is an open access article distributed under the terms and conditions of the Creative Commons Attribution (CC BY) license (<https://creativecommons.org/licenses/by/4.0/>).

1. Introduction

An ultra-wideband (UWB) is a telecommunications technology that is utilized in radio communication networks to achieve high-speed bandwidth connections with minimal energy consumption. Primarily, the UWB was intended for commercial radar. Wireless personal area networks (WPANs) and consumer electronics are two main applications of UWB technology. UWB wireless has developed as an emerging skill with limited smart structures such as radar, wireless communications, and medical engineering domains since its initial achievement in the middle of the 2000s [1]. Until 2001, UWB was significantly

used for military purposes. The Federal Communications Commission (FCC) permitted the public to use UWB bandwidth for commercial purposes after 2002. Furthermore, the FCC approved the usage of the UWB spectrum, which is allocated between 3.1–10.6 GHz in the United States [2]. The low spectral density of UWB is responsible for short range of communication. This function, however, demands high-gain antennas with relatively stable radiation characteristics [3]. Planar antennas, primarily monopoles, are used in UWB electrical devices [4,5] due to its compact size, low profile, and low cost, as well as its ultra-wide impedance bandwidth. Moreover, when these antennas are placed near metallic surfaces, they can cause severe impedance mismatch. Low-profile antennas also transmit limited frequency signals with low gain and poor directivity [6,7].

However, the cost and size of the UWB antennas increases with discreet filters [8]. Frequencies from 5.2–5.8 GHz were notched by etching an omega type slot on the surface of the antenna in [9]. Similarly, in [10], U- and inverted U-shaped slots were embedded in printed monopoles to stop multiple frequencies. A curved shaped slot is introduced in [11] to achieve notching features in WiMAX and WLAN bands. To attain notching characteristics in 5.10–5.94 GHz, an S-shaped slot is applied in the feedline of the monopole antenna in [12]. Split ring resonators can act both as a band stop and band pass filters for different frequencies [13]. In [14], uplink and downlink satellite frequency bands were rejected by introducing a single SRR slot in the patch of the antenna. A WLAN band is rejected by inserting split ring resonators in [15]. Three different frequencies were notched in [16] by embedding multiple split rings near the feedline of the antenna model. Notching was achieved by using SRR in [17]. Tri-notching using frequency-selective surface (FSS) of an ultra-wideband antenna with gain augmentation was reported in [18]. Another compact-sized UWB planar antenna using truncated ground plane was presented in [19]. The antenna covers large bandwidth, but the size was still large, compared to our design. A broadband overleaf-shaped antenna using beam tilt characteristics is presented in [20]. The reported size of the antenna is large, and small bandwidth is achieved, as shown in Table 1. Another Vivaldi antenna resonative over a wide frequency range is reported in [21]. The antenna is antipodal, and the miniaturization was achieved by using exponential strip arms technique.

Table 1. Comparison with the previous research.

Ref. No.	Frequency Range (GHz)	Area (mm ²)	Electrical Size (λ_0^2)	Antenna Type	Substrate Material	Efficiency (%)	Gain (dB)
[11]	3.4–7, 8–11.4	40 × 30	0.94 × 0.705	Split Ring Resonator Patch	FR-4	<95	<5
[12]	3.1–10.6	38.31 × 34.52	0.82 × 0.74	Monopole	FR-4	<95	<5
[13]	4.05–5.1, 6–13	32 × 36	0.89 × 1.01	Circular Patch	FR-4	-	<4
[14]	2.5–19.8	36 × 25	0.62 × 0.43	Slotted Patch	FR-4	-	<3
[15]	2.8–18	50 × 38	0.96 × 0.73	Tapered Slotted Patch	FR-4	-	<4.32
[16]	1.9–5, 6–10.6	48 × 55	0.63 × 0.72	Monopole	FR-4	-	<5
[17]	1.2–9.8	53 × 63.5	0.21 × 0.25	Anti-Spiral Shaped Patch	FR-4	<85	<5.2
[18]	2.6–10.58	38.3 × 34.5	0.33 × 0.3	Sharp triple notched	FR-4	-	<5
[19]	1.5–10.4	64 × 37.4	0.32 × 0.19	Planar patch	F4BM	-	>2
[20]	2–5	100 × 78	0.67 × 0.52	Leaf Shaped Patch	Taconic TLY-5	-	>3
[21]	0.83–9.8	161 × 140	0.45 × 0.39	Ex-potential Strip Arms	$\epsilon_r = 2.3$	-	>2.5
This Work	3–11	25 × 22	0.25 × 0.22	Printed Monopole	FR-4	>85	<4.1

In this research article, a simple CPW based an ultra-wideband antenna having impedance bandwidth ranging from 3 GHz to 11 GHz (8 GHz) for wireless communication networks is presented. It is very hard to achieve a UWB band with compact size; however, in this design, the UWB band is achieved through a CPW technique and the design optimization. The total size of the designed UWB antenna is 25 mm × 22 mm × 1.6 mm. This printed broadband monopole antenna is manufactured using a low-cost FR-4 Duroid

material. The antenna presents good efficiency with suitable gain. This article is organized as follows: the proposed antenna design is presented in Section 2. Results and discussion are presented in Section 3, and the conclusion is given in Section 4.

2. Antenna Design Analysis

The schematic diagram of the designed ultrawideband antenna is presented in Figure 1. The structure of the UWB antenna involves the jug-shaped printed monopole with handle at the right side of the radiator, sized at $L_s \times W_s \times h_s$. The printed monopole is fed by a coplanar waveguide (CPW) feedline of length “ L_f ” and width “ w_f ”. The width of the CPW feedline is kept at 3 mm to attain 50Ω input impedance. The antenna is designed on a low-cost FR-4 substrate having relative permittivity (ϵ_r) of 4.4 and loss tangent ($\tan\delta$) of 0.025. The design is simulated in computer simulation technology (CST-2018) software. On the front view of the substrate, a rectangular ground plane is designed having dimension $L_g \times W_g$, and the ground plane is shown. The three-dimensional (3D) view of the antenna is depicted in Figure 1, and its optimized dimensions are given in Table 2.

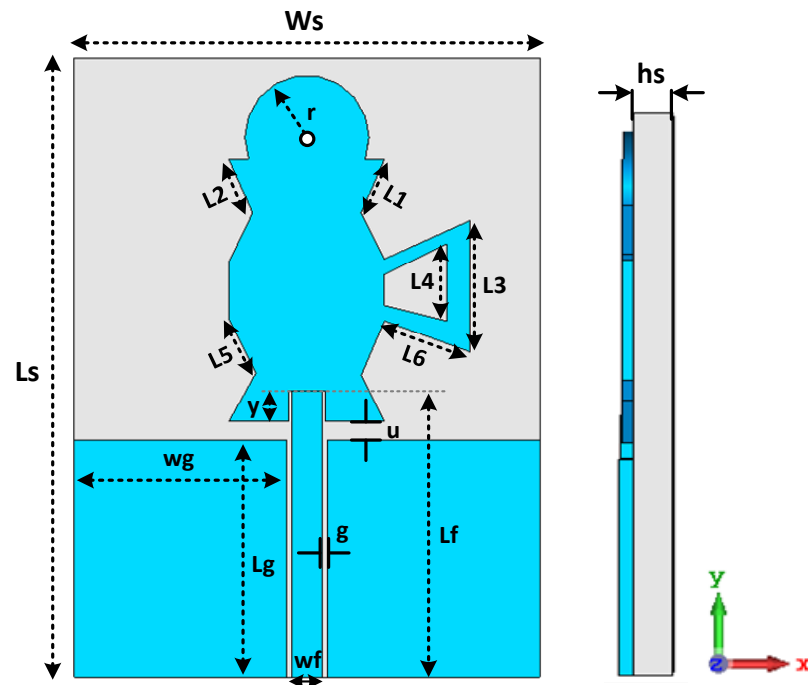


Figure 1. Schematic diagram of the presented UWB antenna.

Table 2. Different design parameters of the presented antenna.

Parameters	Values (mm)	Parameters	Values (mm)
L_s	25	W_s	22
L_f	14.65	W_f	1.58
L_g	12.14	W_g	10.85
L_1	3.02	L_2	2.75
L_3	6.73	L_4	3.96
L_5	3.05	L_6	4.64
g	0.24	y	1.58
u	0.95	h_s	1.6

2.1. Different Design Steps

Figure 2 shows the different design steps of the designed monopole and the S_{11} behavior given in Figure 3. In the first step, the basic design consists of a simple rectangular printed monopole excited by a coplanar waveguide (CPW) feedline, as shown in ANT I. Then, in the second step, the simple rectangular radiator is truncated from its upper and lower sides to keep its shape similar to the body of a jug, which helps to keep the S_{11} (dB) close to -10 dB, but the antenna only operates at 3.5 GHz and 10.5 GHz. Again, in the third step, a semicircular-shaped patch is introduced in the ANT II, which keeps some portion of the UWB band below -10 dB, but the antenna works from 3.3 GHz to 9 GHz and 9.3 GHz to 12 GHz, as can be seen in ANT III (Figure 3), and this is not a required frequency band. Now, in order to achieve the whole UWB spectrum from 3 GHz to 11 GHz, a C-shaped resonator is introduced in the final step to make the shape similar to a handle of a jug, as shown in ANT IV.

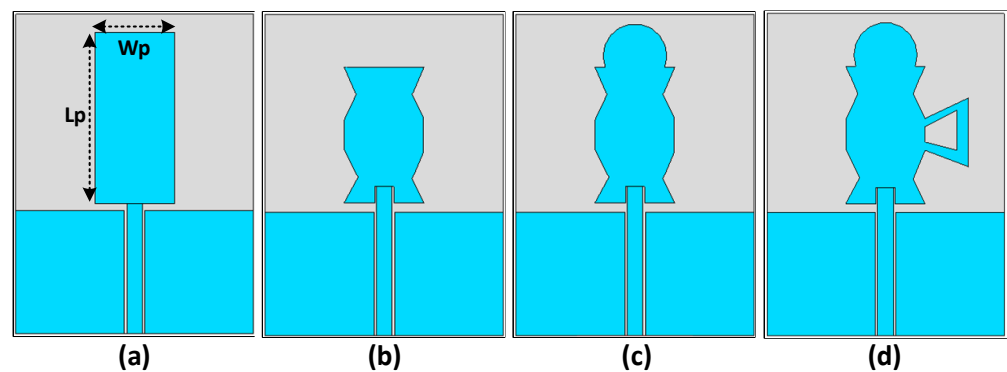


Figure 2. Design steps of the presented ultra-wideband antenna: (a) rectangular printed monopole only (ANT I), (b) truncated monopole (ANT II), (c) addition of semicircular printed monopole (ANT III), (d) presented design (ANT IV).

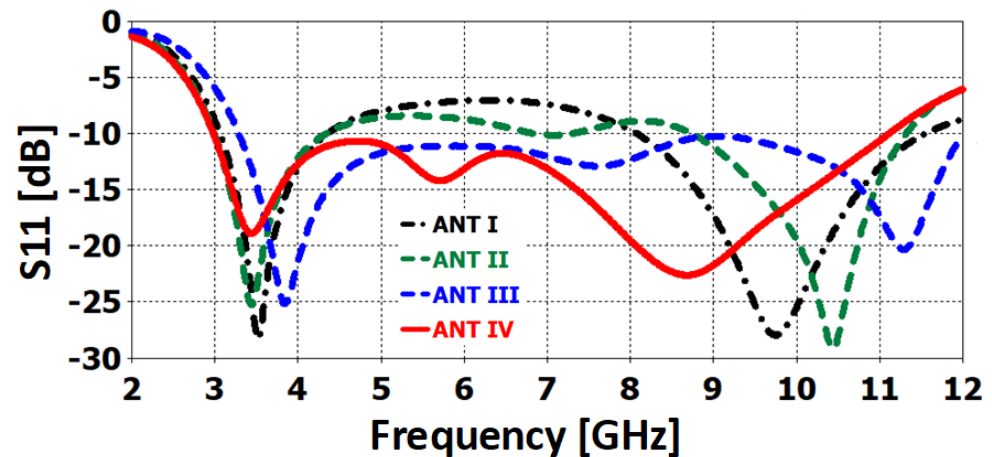


Figure 3. S_{11} (dB) of the different design steps of the presented UWB antenna shown in Figure 2.

The design process of the printed monopole antenna is explained as follows: The primary antenna design (ANT I), shown in Figure 3, contains a 50Ω CPW feedline, a jug-shaped monopole, and the ground plane. The printed monopole's width and length are calculated using Equations (1) and (2) [13], as follows:

$$Wp = \frac{\lambda_0}{2(\sqrt{0.5(\epsilon_r + 1)}} \quad (1)$$

where ϵ_r and λ_o are the relative permittivity and the wavelength of the substrate in free space at the operating frequency. The best option of Wp tends to the perfect impedance matching. The length of the printed monopole can be evaluated by using Equation (2).

$$Lp = \frac{c_o}{2f_o\sqrt{\epsilon_{eff}}} - 2\Delta Lp \quad (2)$$

where c_o , ΔLp , and ϵ_{eff} are the velocity of light, change in the length of the printed monopole due to its fringing effect, and the effective dielectric constant, respectively. The effective relative permittivity can be calculated using Equation (3):

$$\epsilon_{eff} = \frac{\epsilon_r + 1}{2} + \frac{\epsilon_r - 1}{2} \left(\frac{1}{\sqrt{1 + 12 \frac{hs}{Wp}}} \right) \quad (3)$$

where h_{sub} is the height of the substrate. At the end, the fringing effect can be calculated using Equation (4):

$$\Delta Lp = 0.421h_s \frac{(\epsilon_{eff} + 0.300) \left(\frac{Wp}{hs} + 0.264 \right)}{(\epsilon_{eff} - 0.258) \left(\frac{Wp}{hs} + 0.813 \right)} \quad (4)$$

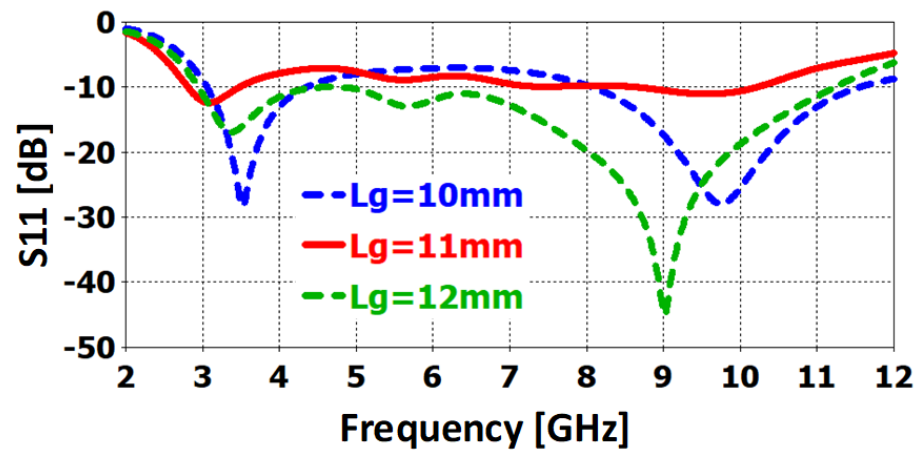
With the placement of $\epsilon_r = 4.3$, $hs = 1.6$ mm in Equations (1)–(4), the initial parameters of the rectangular printed monopole are $Lp = 15$ mm and $Wp = 12$ mm.

With a simple rectangular monopole (ANT I), the antenna works only works at 3.5 GHz and 9.8 GHz, as shown in Figure 3. By ANT II, the bandwidth of the antenna is increased but is unable to achieve UWB band. Then, in the third step (ANT III), with the help of the semicircular printed monopole on the top of the truncated printed monopole, the antenna achieves most of the UWB band, as the antenna has achieved band from 3 GHz to 11 GHz

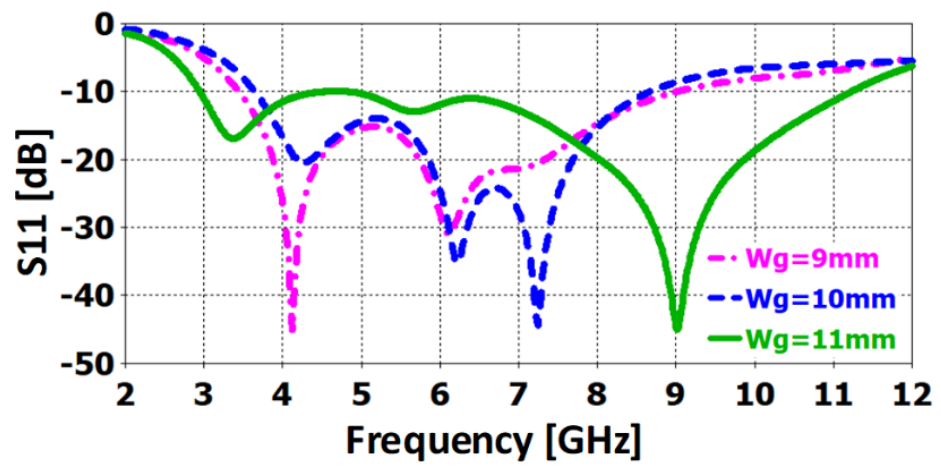
2.2. Parametric Study of the Presented Design

The presented design is finalized after performing several parametric optimizations on different variables, as shown in Figure 4. The first parametric study is performed on the length and width of the ground plane. By increasing the length of the ground plane “Lg” from 10 mm to 12 mm, the impedance matching of the antenna improves with suitable bandwidth, and when the width of the ground plane “wg” is varied from 9 mm to 11 mm, then the bandwidth of the antenna is increased from 4.1 GHz to 8 GHz. The next parametric study is performed on the width of the feedline “wf”. Gradually increasing the width of the feedline improves the impedance bandwidth from 5.8–8 GHz. A parametric study of the C-shaped radiator is also performed. By varying the lengths “L6” and “L3”, the bandwidth of the antenna is improved, as depicted in Figure 4.

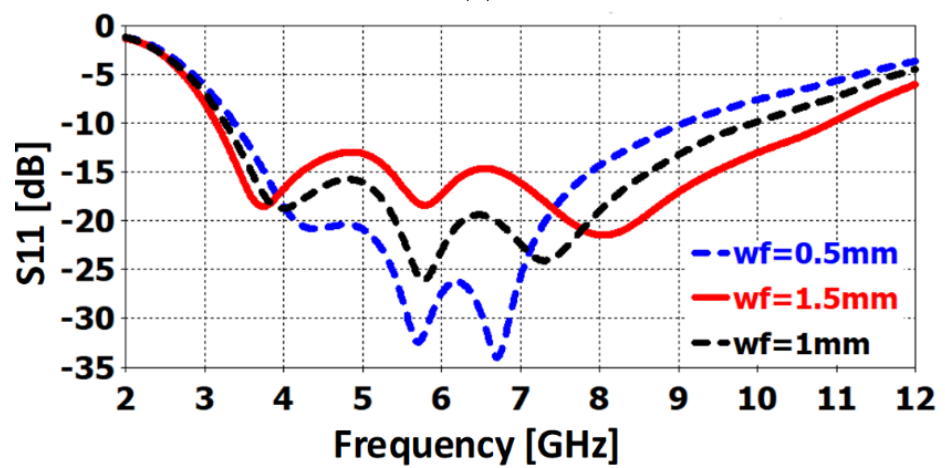
The surface current densities of the UWB antenna at different frequency bands are taken into consideration. This indicates that the antenna plays a significant role in making it resonate at the desired frequency bands. For example, the surface current density at 3.5 GHz is illustrated in Figure 5a. Most of the current seems to flow through the radiator at 3.5 GHz (see Figure 5b), while at 4.1 GHz, the current only flows through the C-shaped resonator and some amount of current through the feedline (see Figure 5c). At 8 GHz, the current flows through the outer lower edge of the printed monopole and some amount of current flow through the CPW ground at 10.5 GHz (see Figure 5d).



(a)

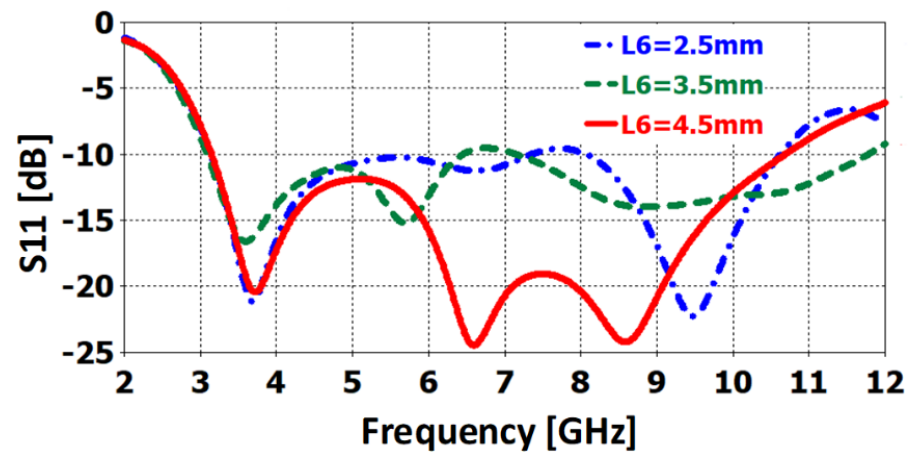


(b)

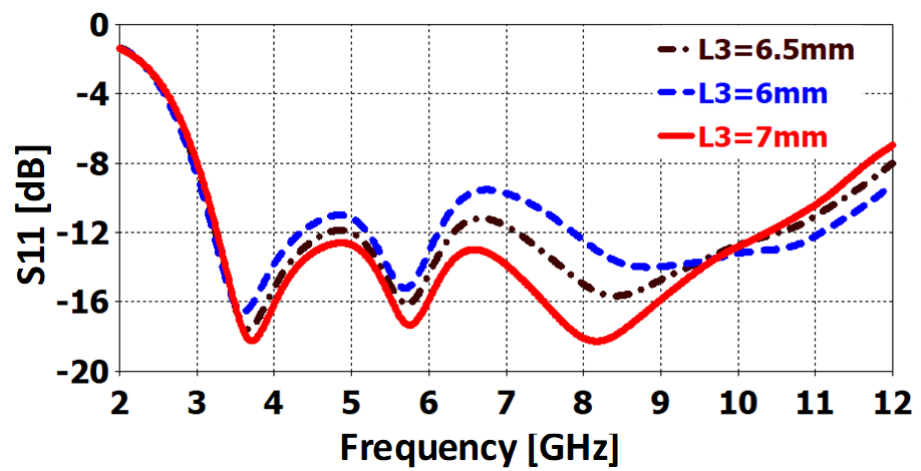


(c)

Figure 4. Cont.



(d)



(e)

Figure 4. Different parameters optimization: (a) variation in “Lg”, (b) variation in “wg”, (c) variation in “wf”, (d) variation in “L6”, (e) variation in “L3”.

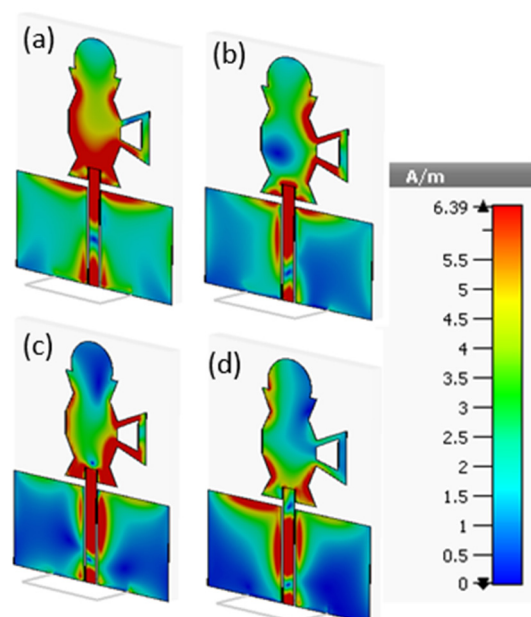


Figure 5. Surface current density (a) at 3.5 GHz, (b) at 4.1 GHz, (c) at 8 GHz, (d) at 10.5 GHz.

2.3. Equivalent Circuit Model

A circuit model for the UWB presented antenna for wireless communications is presented in Figure 6a. The main purpose of the circuit model is to validate the scattering parameters of the ultra-wideband antenna with the S_{11} obtained from the circuit model. The circuit model is designed by using advanced design system (ADS) software. The circuit model consists of four inductors, four capacitors, three resistors, and three resistor-capacitor (RC) circuits connected in series with one resistor and an inductor for each, as given in Figure 6a. By varying the values of the resistors, the S_{11} of the circuit model can be varied, while by fluctuating the values of the capacitors and inductors, the S_{11} of the antenna can be tuned. The values of the lumped components are given in Table 3. The S_{11} (dB) of the circuit model is illustrated in Figure 6b. It covers the bandwidth from 3.1 GHz to 11.5 GHz.

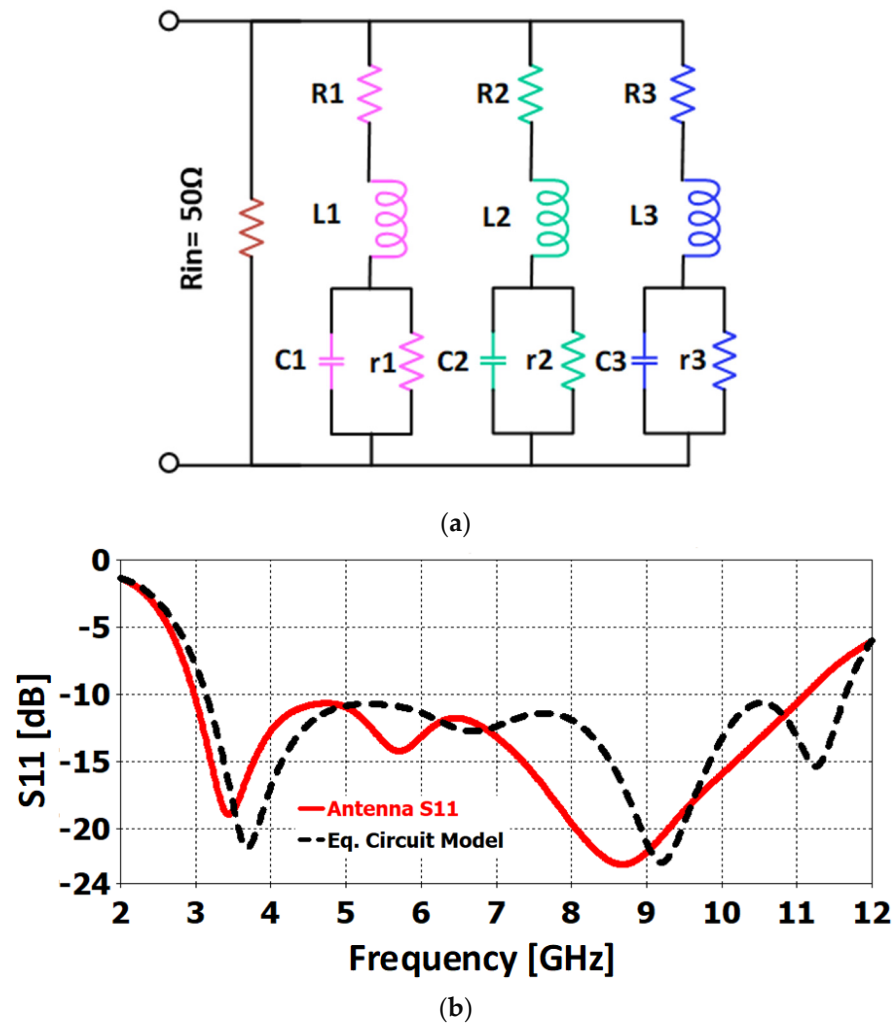


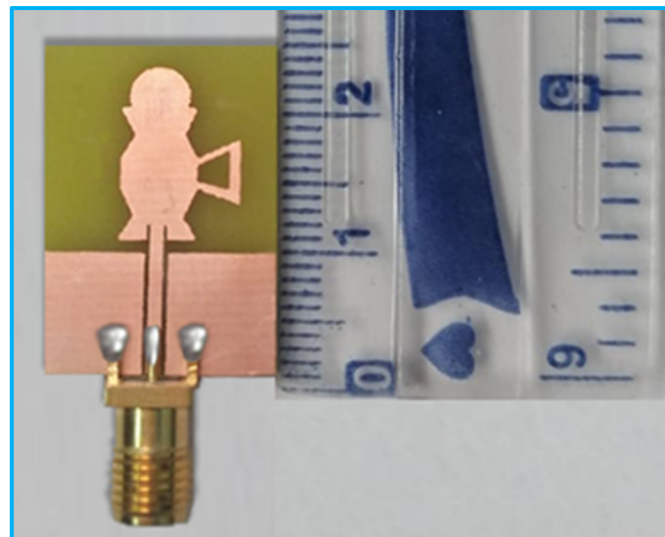
Figure 6. (a) Equivalent circuit model, and (b) reflection coefficient of the equivalent circuit model.

Table 3. Values of the components used in the circuit model.

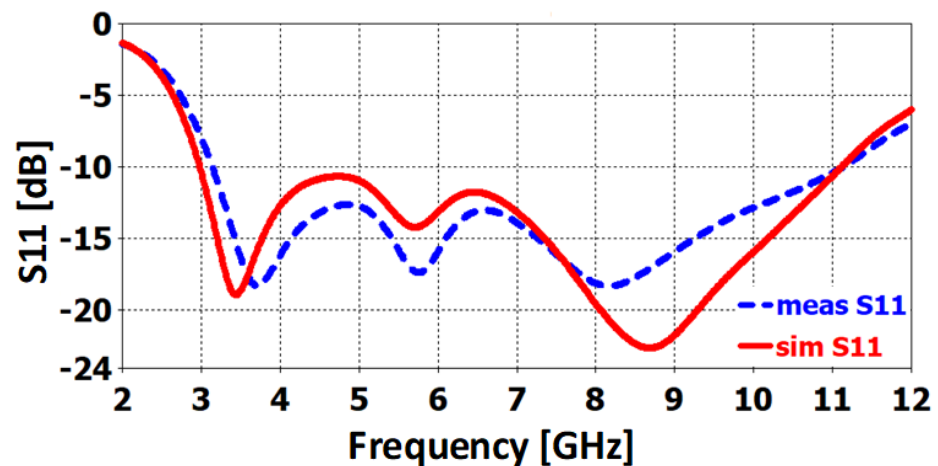
Capacitors	Values (pF)	Inductors	Values (nH)	Resistors	Values (Ω)	High Resistors	Values (Ω)
C1	1	L1	7	R1	2	r1	1500
C2	0.1	L2	0.8	R2	65	r2	1000
C3	0.5	L3	0.5	R3	65	r3	500

3. Results and Discussions

In order to measure the scattering parameters of the fabricated prototype, the port of the fabricated design is connected with a vector network analyzer (VNA). The picture of the prototype is visible in Figure 7a. The S_{11} (dB) of the projected antenna is accessible in Figure 7b. Due to intolerances in the fabrication process and surrounding noises, there are some variations in the measured results. The simulated and measured S_{11} (dB) are in good agreement, as both are covering the whole UWB band for wireless communications.



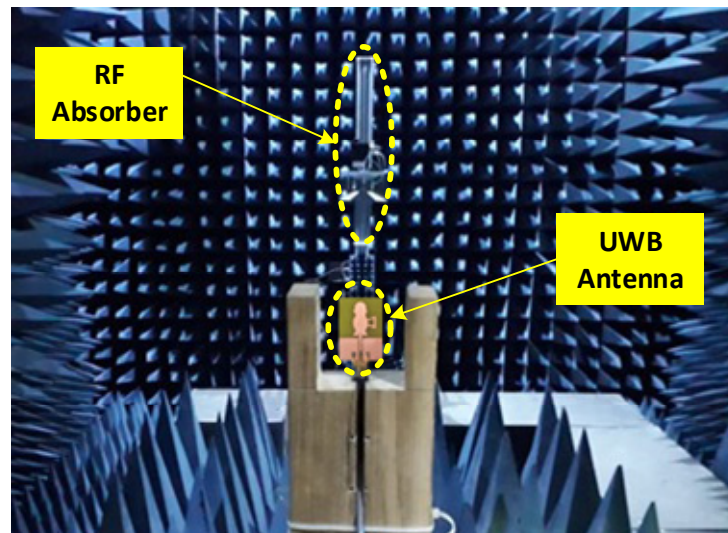
(a)



(b)

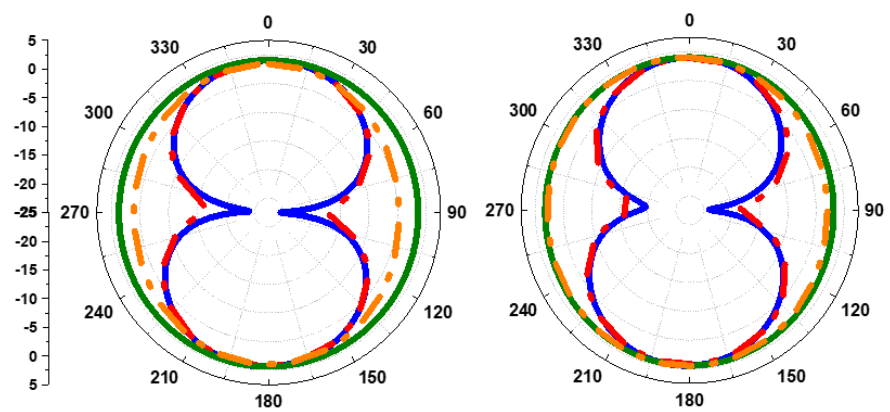
Figure 7. (a) Printed UWB prototype; (b) comparison of simulated and measured reflection coefficients (S_{11}).

The simulated and measured (E & H) plane of the UWB antenna at 3.5 GHz, 4.1 GHz, 8 GHz, and 10.5 GHz are given in Figure 8. It can be seen that there is an omnidirectional pattern at the frequencies of 3.5 GHz and 4.1 GHz along the E-plane while elliptical along the H-plane, and the antenna has a broadside radiation pattern in both planes at the frequencies of 8 GHz and 10.5 GHz. The simulated and measured gain graph is presented in Figure 9. It can be noticed that the antenna has attained the average peak gain ranges from 2–4.1 dB and the antenna's efficiency is attained for more than 85% over the entire band. A comparison with the previous research is given in Table 1.



(a)

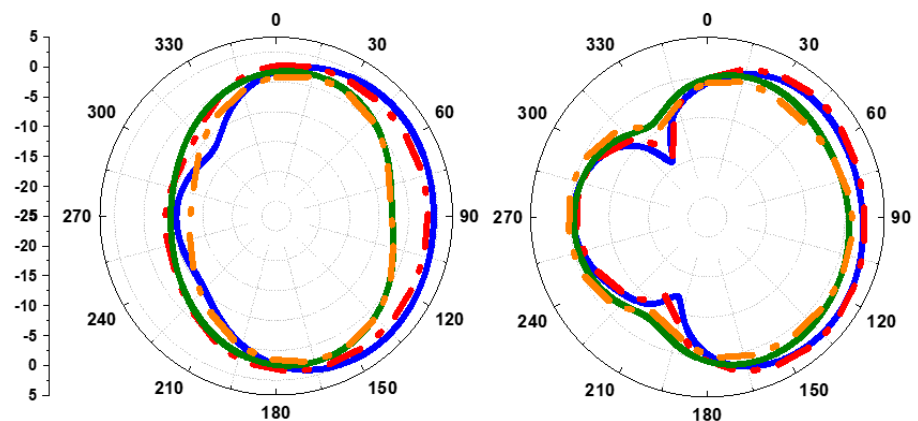
— Sim E-plane, — Meas E-plane, — Sim H-plane, — Meas H-plane



(b)

(c)

— Sim E-plane, — Meas E-plane, — Sim H-plane, — Meas H-plane



(d)

(e)

Figure 8. (a) Simulated and measured 2D radiation pattern setup inside chamber (b) at 3.5 GHz, (c) at 4.1 GHz, (d) at 8 GHz, (e) at 10.5 GHz.

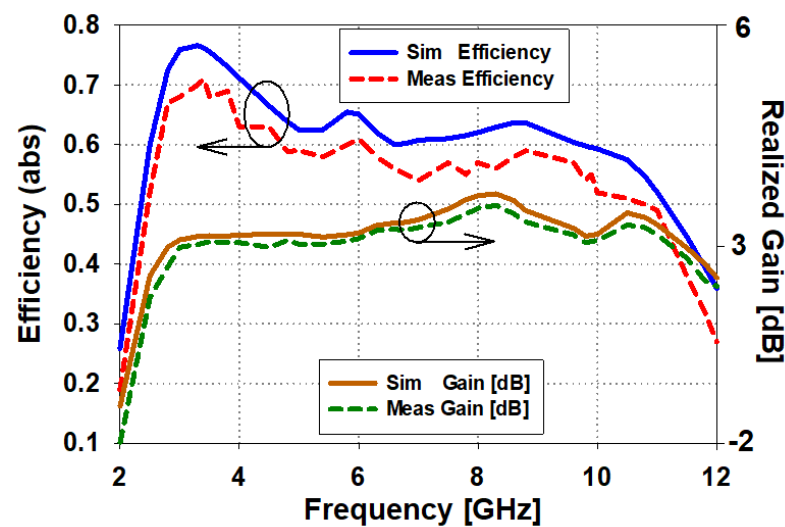


Figure 9. Comparison of simulated and measured efficiency and peak gains (dB).

4. Conclusions

A simple jug-shaped ultra-wideband (UWB) antenna is presented in this work. The presented design is printed, and measured results are also taken. The simulated results are verified by a measured result of the ultra-wideband antenna. The designed UWB antenna is printed on a low-cost FR-4 substrate with relative permittivity of 4.3, loss tangent 0.025, and a standard thickness 1.6 mm, sized at 25 mm × 22 mm × 1.6 mm, suitable for wireless communication system. The designed UWB antenna works with maximum gain (peak gain of 4.1 dB) across the whole UWB spectrum of 3–11 GHz. The simulated and measured reflection coefficients and radiation pattern are in close agreement. The designed antenna is a good applicant for wireless communication systems portable devices.

Author Contributions: Conceptualization, S.A., S.N., M.A.Q. and F.A.; methodology, U.I., A.G. and C.H.S.; software, A.G., S.N. and U.I.; validation, M.A.Q., F.A., U.I. and S.N.; formal analysis, S.A. and A.G.; investigation, A.G., N.O.P. and S.N.; resources, A.G., U.I. and S.A.; data curation, S.A., M.A.Q. and A.G.; writing—original draft preparation, S.A. and A.G.; writing—review and editing, S.N. and F.A.; supervision, N.O.P., C.H.S. and R.A.-A.; funding acquisition, N.O.P., C.H.S. and R.A.-A. All authors have read and agreed to the published version of the manuscript.

Funding: This work received no funding.

Conflicts of Interest: The authors declare no conflict of interest.

References

1. Kirtania, S.; Younes, B.; Hossain, A.; Karacolak, T.; Sekhar, P. CPW-Fed Flexible Ultra-Wideband Antenna for IoT Applications. *Micromachines* **2021**, *12*, 453. [[CrossRef](#)] [[PubMed](#)]
2. Amdaouch, I.; Aghzout, O.; Naghar, A.; Alejos, A.V.; Falcone, F. Design of UWB compact slotted monopole antenna for breast cancer detection. *Adv. Electromagn.* **2019**, *8*, 1–6. [[CrossRef](#)]
3. Saeidi, T.; Ismail, I.; Wen, W.P.; Alhawari, A.R.H.; Mohammadi, A. Ultra-Wideband antennas for wireless communication applications. *Int. J. Antennas Propag.* **2019**, *19*, 7918765.
4. Alhawari, A.; Majeed, S.; Saeidi, T.; Mumtaz, S.; Alghamdi, H.; Hindi, A.; Almawgani, A.; Imran, M.; Abbasi, Q. Compact Elliptical UWB Antenna for Underwater Wireless Communications. *Micromachines* **2021**, *12*, 411. [[CrossRef](#)] [[PubMed](#)]
5. Babale, S.A.; Paracha, K.N.; Ahmad, S.; Abdul Rahim, S.K.; Yunusa, Z.; Nasir, M.; Ghaffar, A.; Lamkaddem, A. A Recent Approach towards Fluidic Microstrip Devices and Gas Sensors: A Review. *Electronics* **2022**, *11*, 229. [[CrossRef](#)]
6. Li, X.-P.; Xu, G.; Ma, M.-R.; Duan, C.-J. UWB Dual-Band-Notched Lanky-Leaf-Shaped Antenna with Loaded Half-Square-Like Slots for Communication System. *Electronics* **2021**, *10*, 1991. [[CrossRef](#)]
7. Rasool, J.M. Ultra Wide Band Antenna Design for Robotics & Sensors Environment. In Proceedings of the 2019 12th International Conference on Developments in eSystems Engineering (DeSE), Kazan, Russia, 7–10 October 2019; pp. 668–672.
8. Iqbal, A.; Smida, A.; Mallat, N.K.; Islam, M.T.; Kim, S. A Compact UWB Antenna with Independently Controllable Notch Bands. *Sensors* **2019**, *19*, 1411. [[CrossRef](#)] [[PubMed](#)]

9. Abbas, A.; Hussain, N.; Lee, J.; Park, S.G.; Kim, N. Triple Rectangular Notch UWB Antenna Using EBG and SRR. *IEEE Access* **2020**, *9*, 2508–2515. [[CrossRef](#)]
10. Abbas, A.; Hussain, N.; Jeong, M.-J.; Park, J.; Shin, K.S.; Kim, T.; Kim, N. A Rectangular Notch-Band UWB Antenna with Controllable Notched Bandwidth and Centre Frequency. *Sensors* **2020**, *20*, 777. [[CrossRef](#)] [[PubMed](#)]
11. Yeboah-Akouwah, B.; Tchao, E.T.; Ur-Rehman, M.; Khan, M.M.; Ahmad, S. Study of a printed split-ring monopole for dual-spectrum communications. *Heliyon* **2021**, *7*, e07928. [[CrossRef](#)] [[PubMed](#)]
12. Alam, M.S.; Abbosh, A. Reconfigurable band-rejection antenna for ultra-wideband applications. *Microw. Antennas Propag. IET* **2018**, *12*, 195–202. [[CrossRef](#)]
13. Abdi, H.; Nourinia, J.; Ghobadi, C. Compact Enhanced CPW-Fed Antenna for UWB Applications. *Adv. Electromagn.* **2021**, *10*, 15–20. [[CrossRef](#)]
14. Upadhyay, A.; Khanna, R. A CPW-fed tomb shaped antenna for UWB applications. *Int. J. Innov. Technol. Explor. Eng. (IJITEE)* **2019**, *8*, 67–72.
15. Hassain, Z.A.A.; Azeez, A.R.; Ali, M.M.; Elwi, T.A. A modified compact bi-directional UWB tapered slot antenna with double band notch characteristics. *Adv. Electromagn.* **2019**, *8*, 74–79. [[CrossRef](#)]
16. Chaudhary, P.; Kumar, A. Compact ultra-wideband circularly polarized CPW-fed monopole antenna. *AEU—Int. J. Electron. Commun.* **2019**, *107*, 137–145. [[CrossRef](#)]
17. Li, X.-P.; Xu, G.; Duan, C.-J.; Ma, M.-R.; Shi, S.-E.; Li, W. Compact TSA with Anti-Spiral Shape and Lumped Resistors for UWB Applications. *Micromachines* **2021**, *12*, 1029. [[CrossRef](#)] [[PubMed](#)]
18. Kundu, S.; Chatterjee, A. Sharp Triple-notched ultra-wideband antenna with gain augmentation using FSS for ground penetrating radar. *Wirel. Pers. Commun.* **2021**, *117*, 1399–1418. [[CrossRef](#)]
19. Guo, L.; Min, M.; Che, W.; Yang, W. A Novel Miniaturized Planar Ultra-Wideband Antenna. *IEEE Access* **2018**, *7*, 2769–2773. [[CrossRef](#)]
20. Delphine, A.; Hamid, M.R.; Seman, N.; Himdi, M. Broadband cloverleaf Vivaldi antenna with beam tilt characteristics. *Int. J. RF Microw. Comput. Eng.* **2020**, *30*, e22158. [[CrossRef](#)]
21. Honari, M.M.; Ghaffarian, M.S.; Mirzavand, R. Miniaturized Antipodal Vivaldi Antenna with Improved Bandwidth Using Exponential Strip Arms. *Electronics* **2021**, *10*, 83. [[CrossRef](#)]